American Mineralogist
Vol. 57, pp. 1614–1642 (1972)

THE EFFECT OF TETRAHEDRAL ANGLES ON Si–O BOND OVERLAP POPULATIONS FOR ISOLATED TETRAHEDRA

S. JOHN LOUISNATHAN AND G. V. GIBBS,
Department of Geological Sciences,
Virginia Polytechnic Institute and State University,
Blacksburg, Virginia 24061

ABSTRACT

Extended Hückel molecular orbitals (EHMO) calculated for orthosilicic acid (D_{2d} symmetry) have the same symmetry as the orbitals in the *ab initio* SCF MO solution; moreover, the calculation yields electronic configuration, relative order of MO energies, and LCAO–MO coefficients that bear a reasonably close similarity with the *ab initio* results (Collins, Cruickshank, and Breeze, 1972). Mulliken (1955) bond overlap populations, n(Si–O), calculated for the hypothetically distorted (C_{3v}, C_{2v}, C_v) silicate ions and orthosilicic acid, with all Si–O = 1.63Å, predict that stronger (shorter) bonds should be involved in the wider tetrahedral valence angles and that weaker (longer) ones should be involved in the narrower angles. The total Hückel energy calculated for the silicate ion as a function of the O–Si–O angles shows a minimum, E_{min}, at the ideal tetrahedral angle of 109.47° when all Si–O distances are equal in length. For a silicate ion (C_{3v} symmetry) with one short apical bond (parallel to C_3) and three long basal bonds, E_{min} results when the three angles involving the short apical bond are wider than the remaining three angles. These predictions are consistent with the experimentally observed steric details. In silicates such steric details are usually associated with polyhedra sharing their elements to form stable crystalline solids. Long Si–O bonds opposite shared edges invariably involve narrow O–Si–O angles whereas short ones opposite unshared edges involve wide angles. The tetrahedral angular distortions and associated Si–O bond length variations observed in $Ba_3Si_4Nb_6O_{26}$, humites, benitoite, sodium metasilicate, and olivines are shown to be qualitatively consistent with the predictions of EHMO theory.

The mean n(Si–O) for distorted tetrahedra is nearly identical with that calculated for a regular one with Si–O = 1.63Å. This may provide justification for Cruickshank's (1961) rule that the average Si–O distance within a silicate ion is ~1.63Å so that as one or more Si–O bonds shorten, the others lengthen so as to preserve the average. The EHMO calculations indicate that accompanying changes in n(Si–O) of individual bonds for distorted tetrahedra there are also variations in the net charges, Q(O), of the oxygen atoms. Using Mulliken's definition of ionic bond orders for heteropolar molecules, it is suggested that the variations in Q(O) may be related to Pauling's (1929) sum of electrostatic bond strengths, ζ(O).

INTRODUCTION

The Si–O bond has been recorded to range in length from 1.51Å in silicon monoxide to 1.78Å in stishovite, while in tetrahedral coordination it shows a somewhat smaller variation from 1.55 to 1.69Å, with a grand mean Si–O tetrahedral distance of ~1.63Å. Moreover, within the same tetrahedron individual bond lengths have been found to vary by as much as 0.12Å even when their estimated standard deviation is less than 0.01Å (Smith and Bailey, 1963). Because the grand mean Si–O tetrahedral distance is considerably shorter than the sum of the single–bond radii (1.83Å), Pauling (1939) proposed a double bond model for the SiO_4 tetrahedron that involves the $3d$ as well as the $3s$ and $3p$ orbitals on silicon. Pauling (1939, 1952) has since shown that such an interpretation would also be more consistent with his electroneutrality principle, because in the double bond model the charge on Si should be less than +1 rather than +2 as in the single bond model or +4 in a purely ionic model. Following Pauling's proposals Cruickshank has since asserted for an ideal (T_d) tetrahedron that two strong π–bonding molecular orbitals are formed with the $3d_{x^2-y^2}$ and $3d_{z^2}$ orbitals (the *e* orbitals) of Si and the appropriate $2p\pi$ and $2p\pi'$ orbitals (the *e* orbitals) of the oxygen atoms; the remaining three $3d_{xy}$, $3d_{xz}$, and $3d_{yz}$ orbitals (the t_2 orbitals) were concluded to be of lesser importance in π–bonding because of their apparent involvement in σ-bonding. This double bonding model has since been substantiated by all–electron *ab initio* self–consistent field molecular orbital (SCF–MO) calculation (Collins, Cruickshank, and Breeze, 1972). Cruickshank's π–bonding model predicts a variable π–bond character that depends in part on the size of the Si–O–Si angle in structures containing polymerized SiO_4 tetrahedra. Investigations by several workers (Cruickshank, 1961; Lazarev, 1964; McDonald and Cruickshank, 1967; Cannillo, Rossi, and Ungaretti, 1968; Bokii and Struchkov, 1968; Brown, Gibbs, and Ribbe, 1969; Brown and Gibbs, 1970; Louisnathan and Smith, 1971; Gibbs *et al.*, 1972) suggest that the mobile bond order of the Si–O(br) bond is perturbed by the size of Si–O–Si angle, with shorter bonds tending to be associated with wider angles in silicates and siloxanes. In addition to such a variable π–bond character, the following factors have been suggested as being important in affecting the Si–O bond length variation: (1) the coordination number of oxygen, CN(O), (2) the CN of cations bonded to oxygen, (3) the valence of cations bonded to oxygen, (4) the mean cation–oxygen distance, and (5) the mean electronegativity of the cations bonded to oxygen, $\bar{\chi}$(O). The effect of CN(O) on the Si–O bond length has been investigated by Brown and Gibbs (1969) who find that larger *mean* CN(O) is associated with longer *mean* Si–O bond length; however, they note that the *actual* CN(O) does not, in general, show a simple trend with *individual* Si–O distances. Factors (1), (2), (3), and, to a certain extent, (4) are used to characterize Pauling's ζ(O), the sum of electrostatic bond strength reaching an oxygen. Baur (1970 and 1971) has shown that the correlation between the Si–O bond length and $\zeta(O)$ is so well–developed that it can be used to "predict" bond lengths with a fairly high precision, providing the oxygen atoms in a structure are not all charge–balanced. The effect of $\bar{\chi}(O)$ on Si–O bond length has been studied by several investigators (Noll, 1963; McDonald and Cruickshank, 1967; Brown and Gibbs, 1970; Mitchell, Bloss, and Gibbs, 1971) who find that the correlation between $\bar{\chi}(O)$ and Si–O distances is fairly well–developed in selected structurally related compounds, while such correlations do not appear to be important in other topologically related structures (Novak and Gibbs, 1971; Baur, 1971; Brown and Gibbs, in prep.). It must be remarked that the relationship between electronegativity and bond length is much more complex than commonly believed.

There are a number of cases where neither the simple π–bonding scheme nor the electrostatic model based on $\zeta(O)$ adequately account for the variation in individual Si–O bond lengths. The Si–O bond length variation in olivine is such an example. The main purpose of our paper is to examine the variation of the Si–O bond strength as a function of tetrahedral angle, and to offer a hitherto neglected mechanism, namely, the induced angular distortion in the O–Si–O angles, as a possible and, in many cases, perhaps a primary cause for the variation of the Si–O bond length.

In the last few years, semi–empirical extended Hückel molecular orbital (EHMO) calculations have made a significant contribution to our understanding of the valence theory of organic and inorganic molecules by satisfactorily predicting their conformational geometries[1] despite the very crude nature of the method (Hoffmann, 1963; Allen and Russell, 1967). In addition, Boyd and Lipscomb (1969) and more recently Bartell, Su, and Yow (1970) and Gibbs, Hamil, Louisnathan, Bartell, and Yow (1972) have made similar calculations for selected PO_4, SO_4, and SiO_4 containing molecules and found that their results fairly successfully account for *trends* in the observed tetrahedral bond lengths. Since we are interested in conformational predictions for the SiO_4 tetrahedron, we shall employ the EHMO method for a series of hypothetical ideal and distorted SiO_4 tetrahedra (Louisnathan and Gibbs, 1971).

THE LCAO–EHMO THEORY

The EHMO method is an extension of the well known π–electron Hückel theory (*cf.* Salem, 1966) designed to include both the σ– and

---

[1] The geometry that a three dimensional molecule adopts in its ground state.

the π–electrons. All calculations presented in our paper were obtained using the EHMO program originally written by Hoffmann (1963). In these calculations, one–electron MO wave functions are constructed as a linear combination of n basis atomic orbitals (AO),

$$\Psi_k = \sum_j^n c_{kj}\phi_j \tag{1}$$

where c_{kj} are the LCAO–MO coefficients and the ϕ_j are Slater type atomic orbitals (STO–AO). However, only the valence orbitals of an atom are used in the construction of Ψ_k; *e.g.*, for an oxygen atom this would include its $2s$, $2p_x$, $2p_y$, and $2p_z$ orbitals. The c_{kj} are obtained from a set of simultaneous secular equations, where

$$\sum_{i=1}^n (H_{ij} - \epsilon_k S_{ij})c_{kj} = 0, \qquad j = 1, 2, 3, \cdots, n, \tag{2}$$

where

$$S_{ij} = \int \phi_i\phi_j \, d\tau \tag{3}$$

are the overlap integrals explicitly evaluated for the STO centered on the appropriate atoms and where H_{ij}, the Hamiltonian matrix elements, are undefined but are assumed to be proportional to the overlap integrals S_{ij} (Mulliken, 1955) following the Wolfsberg–Helmholz (1952) parametrization,

$$H_{ij} = K[H_{ii} + H_{jj})/2]S_{ij}. \tag{4}$$

In this expression, K is an empirical constant ($K = 2.0$ in all our calculations) and H_{ii} are assumed to equal the negative of the valence orbital ionization potentials (VOIP) of ϕ_i. The one–electron MO energies, ϵ_k, are found by diagonalizing the secular determinant

$$|H_{ij} - \epsilon S_{ij}| = 0 \tag{5}$$

and the set of coefficients c_{kj} corresponding to the Ψ_k MO (1) are obtained by inserting each ϵ_k into (2) and solving the resulting simultaneous secular equations. The Ψ_k are then filled with electrons pairwise starting with the lowest eigenstate, ϵ_k, in conformity with the Pauli exclusion and *aufbau* principles. The total electronic energy for a closed–shell molecule is assumed to equal the sum of the eigenstate energies of the MOs

$$E = \sum_k \epsilon_k N_k \tag{6}$$

where N_k(0, 1, or 2) is the number of electrons in the kth eigenstate. This energy, E, referred to as the total Hückel energy of the molecule, does not equal the true total energy, W, but represents to a first approximation the kinetic energy plus twice the repulsive Coulomb and electron–electron exchange interactions, V_{ee}, of the valence electrons (Slater, 1963). To obtain W, we must add to E, (1) the energy of core electrons, and (2) the nuclear framework electrostatic repulsive energy, V_{nn}, and (3) subtract one magnitude of V_{ee} which was counted twice:

$$W = \sum_{k}^{\text{valence}} \epsilon_k N_k + \left(\sum_{k}^{\text{core}} \epsilon_k N_k + V_{nn} - V_{ee} \right). \tag{7}$$

In *ab initio* SCF MO calculations, an iterative procedure guarantees that the calculation of the total energy be close to true W (*cf.* Richards and Horsley, 1970). In the EHMO calculations, the terms in the parentheses of equation (7) are completely neglected. The neglect of electrostatic interactions is a serious handicap in the EHMO method, especially for molecules or complexes where cation–cation repulsions are large. However, there are cases where the Hückel E closely simulates the behavior of the true nonrelativistic energy W because (1) the choice of VOIP and the Wolfsberg–Helmholz parametrization for the Hamiltonians introduces a certain amount of nuclear repulsive energy into calculation and (2) to a very rough approximation V_{nn} and V_{ee} may, in part, cancel one another (Slater, 1963; Hoffmann, 1963). When this is true, the energy of core electrons behaves to a first approximation as a constant in a set of calculations for a given molecule. In a review of the strengths and weaknesses of the EHMO method, Allen (1970) has pointed out that when the electronegativity difference between a bonded pair of atoms in a molecule exceeds 1.3 (Pauling's scale) the criterion of E simulating W starts to break down. In fact, in the case of a molecule like Li_2O where the electronegativity difference is 2.5, breakdown of the method is complete in that there are virtually no correspondences with results obtained by *ab initio* methods.

Using the calculated atomic orbital overlaps, S_{ij}, and the LCAO–EHMO coefficients c_{ik}, the orbital charges (q_j), the bond overlap populations between atoms r and s, $n(r\text{–}s)$, and the net atomic charges, $Q(r)$ were calculated using Mulliken's (1955) recipes. The bond overlap population for the Si–O bond is thus calculated from

$$n(\text{Si–O}) = \sum_{k} \sum_{i,j} 2N_k c_{ki(\text{Si})} c_{kj(\text{O})} S_{\text{Si}(i)\text{O}(j)}. \tag{8}$$

The non-bonded geminal populations, $n'(r\text{–}s)$, were calculated from the $O\cdots O$ overlap populations following a procedure outlined by Bartell *et al.* (1970). For a SiO_4 tetrahedron the geminal population in a given bond Si–O_l ($l = 1, 2, 3$, or 4, the subscripts for the four oxygen atoms) is given by

$$n'(\text{Si–O}_l) = \sum_{m \neq l} n(\text{O}_l \cdots \text{O}_m) \tag{9}$$

where $n(O_l\cdots O_m)$ is the overlap population in the $O_l\cdots O_m$ non-bonded internuclear direction; $n(O\cdots O)$ are generally negative numbers.

The bond overlap populations, the geminal populations, the net atomic charges, *etc.* calculated in the EHMO approximation are *not* absolute. However, the *trends* shown by these quantities in a series of molecules or ions appear to conform with experimentally observed trends in bond length variation. The bond overlap population $n(r–s)$ is a measure of the strength of the bond $r–s$; if $n(r–s)$ is positive, atoms r and s are considered bonded, if zero, r and s are non–bonded and if negative, r and s are antibonded. The geminal population, $n'(r–s)$, is a measure of nonbonded repulsions in a bond. In a silicate ion, for example, $n'(\text{Si–O}_1)$ would represent the non–bonded repulsions arising from $O_1\cdots O_2$, $O_1\cdots O_3$ and $O_1\cdots O_4$, and as $n'(\text{Si–O}_1)$ becomes more negative the repulsions increase and Si–O_1 would tend to lengthen with respect to the other three bonds.

EHMO CALCULATIONS

The VOIP used to generate the Hückel Hamiltonian matrix, and the STO exponents, $\xi(\phi_j)$, used to calculate the overlap matrix, are listed in Table 1. Calculations were undertaken for the following ideal (T_d and D_{2d}) and distorted (C_{3v}, C_{2v}, and C_v) silicate ions and orthosilicic acid molecules:

1. Silicate ion (T_d – point symmetry) with Si–O = 1.63Å, and *sp* and *spd* basis sets on Si (Fig. 1a);
2. Orthosilicic acid (T_d), with *sp* and *spd* basis sets on Si and Si–O separation at various lengths between 1.5 and 1.7Å. (Fig. 1b);
3. Orthosilicic acid with D_{2d} symmetry (same conformation as used by Collins *et al.* (1972) in their *ab initio* SCF MO calculation) where all O–Si–O and Si–O–H angles were assumed to be 109.47°, Si–O = 1.62, and O–H = 0.96Å.
4. Orthosilicic acid (C_{3v}, Si–O = 1.63Å, *spd* basis set on Si) with all Si–O–H linkages linear (Fig. 1c), and three basal H atoms in an edge–sharing configuration and the apical H making a linear (Fig. 1d) or bent (Fig. 1e) Si–O–H linkage;

Table 1. VOIP and STO exponents used in the EHMO calculations*

Orbital	VOIP	ξ
H 1*s*	13.60 eV.	1.200
O 2*s*	32.33	2.246
2*p*	15.79	2.227
Si 3*s*	14.19	1.643
3*p*	8.15	1.428
3*d*	5.50	1.000

* All VOIP values are chosen similar to those given by Basch, Viste and Grey (1965) and Slater exponents are SCCC values from Clementi and Raimondi (1963), except for Si(3*d*) for which the values were taken to correspond with those used by Gibbs *et al.* (1972).

5. Orthosilicic acid (C_{3v}, Si–O = 1.63Å, *spd* basis set on Si) where the apical (α) and basal (β) O–Si–O angles were varied within the constraints of C_{3v} point symmetry;
6. Orthosilicic acid (C_{2v}, Si–O = 1.63Å, *spd* basis set on Si) for two combinations of O–Si–O angles (Fig. 1f);
7. Orthosilicic acid (C_v, Si–O = 1.63Å, *spd* basis set on Si) with O–Si–O angles similar to those observed in the olivines (Brown and Gibbs, in prep.). In one calculation the Si–O–H linkages are linear (Fig. 1g) and in the other the three basal H atoms form exactly the same configuration that *M*-site cations make around the SiO_4 group in forsterite, while the apical H is placed at 2.089Å, the mean O(1)–*M* distance in forsterite (Fig. 1h); and
8. Silicate ion with point symmetries C_{3v}, C_{2v}, and C_v, and the O–Si–O angles given in Fig. 1d, 1f, and 1g respectively, with and without 3*d* orbitals on Si.

RESULTS AND DISCUSSION

In discussing the energies and strengths of covalent bonds, Pauling (1939, 1960) introduced the criterion of maximum overlapping which states *"that of two orbitals in an atom the one that can overlap more with an orbital of another atom will form the stronger bond with that atom, and, moreover, the bond formed by a given orbital will tend to lie in that direction in which the orbital is concentrated."* Mulliken (1950) has also suggested that a logical measure of bond strength should be the overlap integral itself because it includes both the radial and angular portions of the AO wavefunctions (cf. Fyfe, 1954; Cotton and Wilkinson, 1966). More recently, however, he (1955) proposed that overlap populations, $n(r\text{–}s)$, are a better measure of the strength of a covalent bond between two atoms, r and s, because $n(r\text{–}s)$ take proper account of the overlaps with respect to bonding as well as nonbonding and antibonding effects in the MOs. For this reason we will use overlap populations in our paper as the primary criterion for ordering and classifying variations in bond lengths. The actual numerical value calculated for $n(r\text{–}s)$ cannot be regarded as indicating the actual number of electrons located in the region between r and s; however, it can be considered as an index of binding (Coulson, 1970).

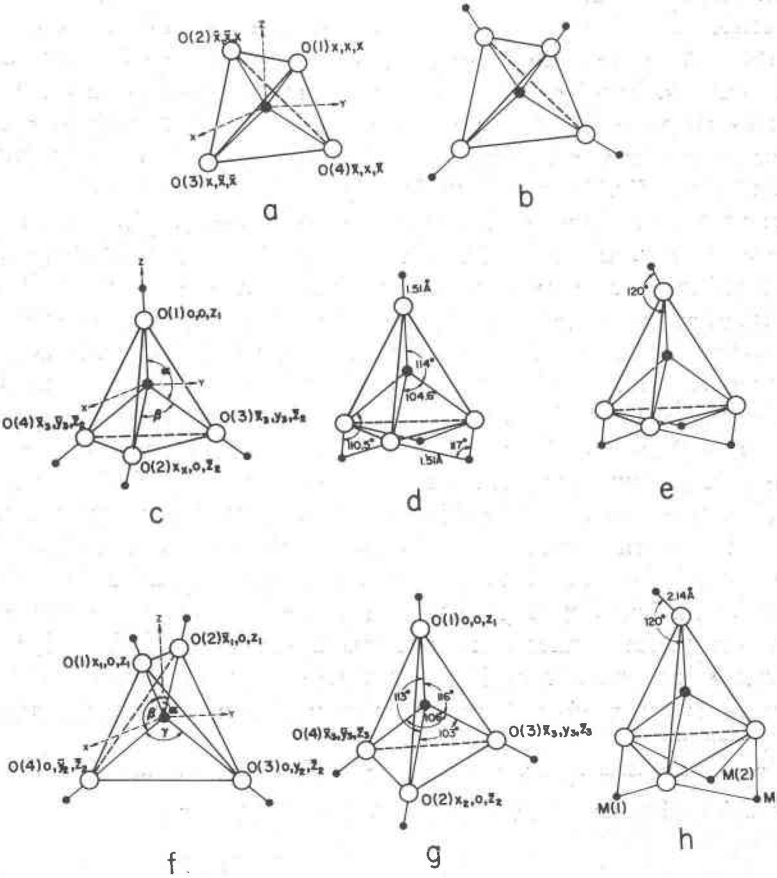

FIG. 1. Coordinate systems and geometries of silicate ions and orthosilicic acid molecules investigated (see text for details). Open circles represent O atoms, large filled circles Si, and small filled circles H. The C_n axes are always chosen along the z coordinate axis. All Si–O = 1.63Å and all Si–H 1.0Å unless otherwise specified.

THE SILICATE ION AND ORTHOSILICIC ACID (T_d AND D_{2d} POINT SYMMETRY)

The electronic configuration of the valence electrons and the MO energies (ϵ_k) obtained in our EHMO calculations are listed in Table 2 along with those obtained in the *ab initio* SCF–MO calculations by Collins *et al.* (1972). In spite of the drastic assumptions involved in extended Hückel theory, there is in general a *qualitative* agreement in the electronic configuration and the *relative* order of ϵ_k between the *ab initio* and EHMO results. In the Si(*spd*) calculation for orthosilicic acid (D_{2d}) symmetry, the ϵ_k (EHMO) of the lower strongly bonding orbitals ($4a_1$ to $1b_1$) are identical in their relative order to the ϵ_k (*ab initio*). There are some reversals in the top weakly bonding ($5b_2$ and $6e$) and non-bonding ($1a_2$) orbitals. Despite the lack of any sort of iterations in the EHMO computation, the LCAO–MO coefficients appear to be fairly well correlated with those obtained in the *ab initio* calculation (Fig. 2) suggesting that the MO's of the extended Hückel approximation have qualitatively the same spatial distribution as those of *ab initio* SCF–MOs. Likewise, the Si(*sp*) calculation for the orthosilicic acid bears a qualitative resemblance with the *ab initio* calculation except that the relative order of $3e$ and $3b_2$ are reversed. However, because ϵ_k (EHMO) of $3e$ and $3b_2$ are nearly identical, such a reversal will not seriously affect the calculated n(Si–O). For the silicate ion, the *ab initio* calculations yield positive values of ϵ_k for most of the valence orbitals in contrast to the negative values obtained in the EHMO approximation. On the other hand, the EHMO results (ϵ_k, c_{kj}, $n(r\text{–}s)$, etc.) for the silicate ion bear a qualitative resemblance with the *ab initio* results and a strong resemblance with the EHMO results for the orthosilicic acid molecule. Such a resemblance, which may be attributed in large part to the neglect of electron–electron and nuclear–nuclear Coulomb and exchange interactions in EHMO theory, suggests that *trends* in n(Si–O) for a series of silicate tetrahedra may not be seriously affected by the omission of non–tetrahedral cations of a structure.

The bond overlap populations n(Si–O) obtained in our calculations for a Si–O distance of 1.63Å and O–Si–O = 109.47° are:

	basis set	
	Si(*sp*)	Si(*spd*)
Orthosilicic acid (D_{2d})	0.466	0.750
Orthosilicic acid (T_d)	0.514	0.857
Silicate ion (T_d)	0.496	0.906

Table 2. Electronic configuration (C) and MO energies (ε_k) in e.V. for the $(SiO_4)^{4-}$ ion and the H_4SiO_4 molecule.

	$(SiO_4)^{4-}$ (T_d)								H_4SiO_4 (D_{2d})								H_4SiO_4 (T_d)			
	SCF-MO[1]		EHMO		SCF-MO		EHMO		SCF-MO		EHMO		SCF-MO		EHMO		EHMO		EHMO	
	(sp)		(sp)		(spd)		(spd)		(sp)		(sp)		(spd)		(spd)		(sp)		(spd)	
	C[2]	ε_k	C	ε_k	C	ε_k	C	ε_k	C	ε_k	C	ε_k	C	ε_k	C	ε_k	C	ε_k	C	ε_k
Valence MOs									$6e$	-6.91	$6e$	-15.45	$1a_2$	-7.43	$6e$	-15.59				
	$1t_1$	+27.21	$5t_2$	-15.53	$1t_1$	+20.54	$1t_1$	-15.60	$1a_2$	-6.96	$5b_2$	-15.57	$6e$	-8.65	$5b_2$	-15.60	$1t_1$	-15.61	$1t_1$	-15.61
									$5b_2$	-7.43	$1a_2$	-15.60	$5b_2$	-9.98	$1a_2$	-15.60				
	$5t_2$	+27.21	$1t_1$	-15.61	$5t_2$	+18.01	$5t_2$	-15.61	$1b_1$	-7.97	$1b_1$	-15.91	$1b_1$	-11.78	$1b_1$	-16.40	$5t_2$	-15.84	$5t_2$	-16.28
									$6a_1$	-12.87	$5e$	-16.38	$5e$	-14.12	$5e$	-16.66				
	$1e$	+26.14	$1e$	-15.90	$1e$	+14.91	$1e$	-16.39	$5e$	-13.03	$6a_1$	-16.54	$6a_1$	-14.64	$6a_1$	-16.80	$1e$	-15.90	$1e$	-16.39
									$4e$	-14.36	$4e$	-17.37	$4e$	-15.75	$4e$	-17.70				
	$4t_2$	+20.08	$4t_2$	-16.38	$4t_2$	+12.73	$4t_2$	-16.67	$4b_2$	-17.19	$4b_2$	-18.55	$4b_2$	-18.12	$4b_2$	-18.56	$4t_2$	-18.16	$4t_2$	-18.23
	$5a_1$	+16.54	$5a_1$	-17.27	$5a_1$	+10.28	$5a_1$	-17.27	$5a_1$	-18.66	$5a_1$	-18.96	$5a_1$	-19.23	$5a_1$	-18.98	$5a_1$	-19.96	$5a_1$	-19.96
									$3b_2$	-40.75	$3e$	-33.89	$3b_2$	-42.30	$3b_2$	-33.94				
	$3t_2$	-4.95	$3t_2$	-32.75	$3t_2$	-13.19	$3t_2$	-32.96	$3e$	-40.83	$3b_2$	-33.93	$3e$	-42.33	$3e$	-33.94	$3t_2$	-33.87	$3t_2$	-33.88
	$4a_1$	-6.15	$4a_1$	-34.95	$4a_1$	-14.15	$4a_1$	-34.95	$4a_1$	-41.76	$4a_1$	-35.65	$4a_1$	-43.12	$4a_1$	-35.68	$1a_1$	-35.58	$4a_1$	-35.58
Valence $\sum_k \varepsilon_k N_k$		+542.64		-649.66		+280.44		-655.07		-607.70		-674.18		-656.60		-678.70		-675.55		-680.61

---

[1] Refers to all electron *ab initio* SCF MO calculation (Collins, Cruickshank and Breeze, 1972); (*sp*) refers to a minimum-basis-set, and (*spd*) refers to addition of two sets (diffuse and contracted) of *d*-type functions on silicon. The calculations used STOs each expanded by three Gaussian-type functions. Low energy non-valence orbitals have been omitted from the list (*loc. cit.*).

[2] C = electronic configuration; each MO contains two electrons; MOs of T_1 and T_2 representations are triply degenerate in T_d group and those of E representation are doubly degenerate in both T_d and D_{2d} groups.

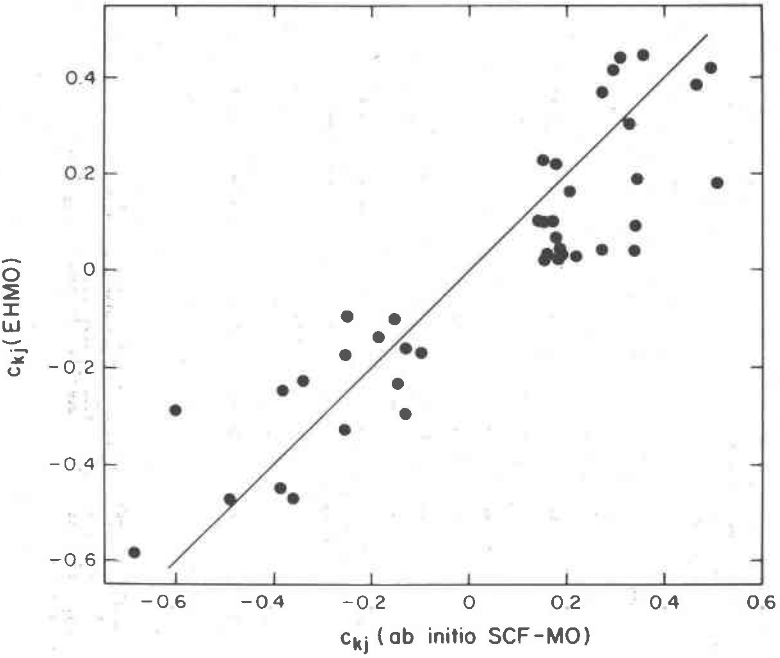

FIG. 2. A plot of LCAO-MO coefficients, Si(*spd*) basis, obtained in the EHMO calculations versus those obtained in the *ab initio* SCF-MO calculations of Collins *et al.* (1972). Coefficients less than 0.1 are omitted. The solid line indicates the expected (45°) slope.

Bending the Si–O–H angle (180° in T_d and 109.47° in D_{2d}) has a relatively large effect on the n(Si–O); larger populations are calculated for the linear linkage predicting a shorter Si–O bond length for the T_d conformation than for the D_{2d} conformation of orthosilicic acid. In discussing bond length changes, it would be convenient if we could estimate bond length variations from the calculated overlap populations. Mulliken (1955) has suggested that the change Δr in the equilibrium bond length, r_e, in a molecule upon removal of an electron should be proportional to the change Δn in the equilibrium overlap population, n_e. A plot of $[-\Delta n(\text{Si–O})/n_e(\text{Si–O})]$ versus $[\Delta r(\text{Si–O})/r_e(\text{Si–O})]$, with n_e(Si–O) taken as the value obtained for the orthosilicic acid with T_d symmetry of assumed r_e(Si–O) = 1.63Å and Δn obtained from the EHMO calculations in which the Si–O bond length was varied from 1.5 to 1.7Å, is shown in Figure 3. In this figure data points from both Si(*sp*) and Si(*spd*) basis set calculations plot close to the 45° line suggesting that the relation

$$-\frac{\Delta n}{n_e} = \frac{\Delta r}{r_e} \tag{10}$$

may be used to give a very crude estimate of bond length changes. Strictly speaking this equation should be only valid when the symmetry of orthosilicic acid is close to T_d (*i.e.*, all tetrahedral angles close to 109.5°). As O–Si–O angular distortions increase, n_e and r_e may not be equal-valued for all four bonds in a (SiO_4) group and will increasingly deviate from the values obtained for an ideal tetrahedron.

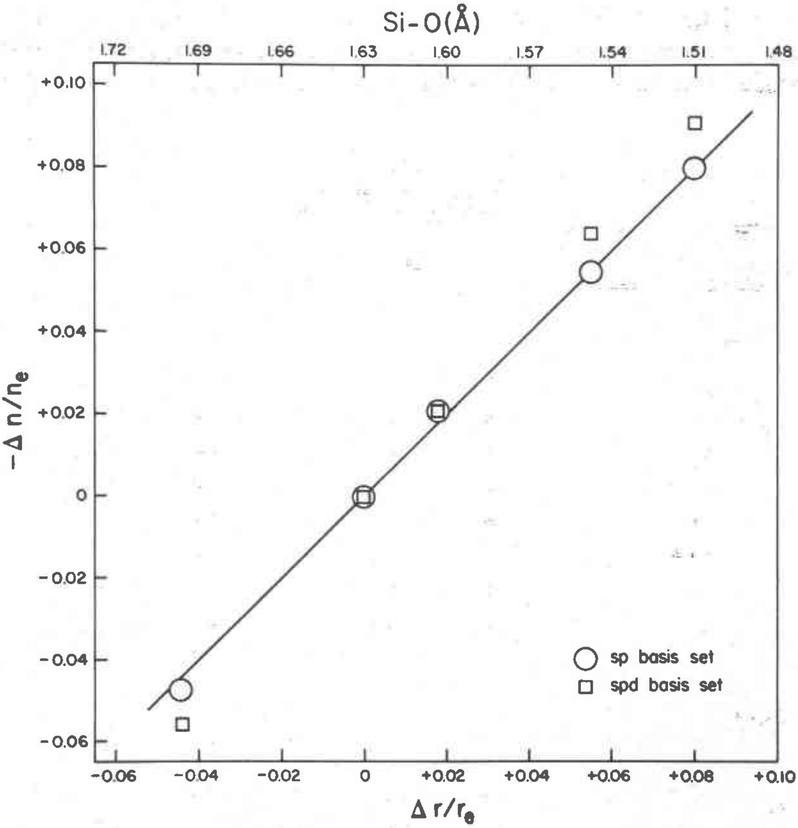

FIG. 3. A plot of ($-\Delta n/n_e$) *versus* ($\Delta r/r_e$) assuming $n_e = 0.514$ (in Si(*sp*) basis) or 0.857 (in Si(*spd*) basis) as obtained for the H_4SiO_4 molecule (T_d symmetry) where $r_e = 1.63$Å.

ORTHOSILICIC ACID (C_{3v} POINT SYMMETRY)

The n(Si–O) and n'(Si–O) values calculated for a series of orthosilicic acid molecules with C_{3v} point symmetry are listed in Table 3. When α = O(apical)–Si–O(basal) angles (see Fig. 1c) are wider than β = O(basal)–Si–O(basal) angles, the overlap population of apical bond is larger than that of the basal bonds. When β is larger than α the n(Si–O) of basal and apical bonds are reversed with n[Si–O(basal)] > n[Si–O(apical)]. The geminal populations n'[Si–O(apical)] also increase as α decreases. These results suggest that when the SiO_4 tetrahedron possesses C_{3v}–type angular distortions with α larger than β, conformational stabilization should occur requiring that the basal bonds lengthen and the apical bond shorten relative to the Si–O distance in the ideal tetrahedron.

In Figure 4 the n[Si–O(apical)] and n[Si–O(basal)] are plotted as a function of the O(apical)–Si–O(basal) angle (α). As the three α angles associated with Si–O(apical) bond widen, the overlap popula-

Table 3. Bond overlap populations, n(Si-O), and non-bonded geminal populations, n'(Si-O) for the ideal and distorted (SiO_4)-tetrahedra (Si-O = 1.63Å, spd basis set on Si).

Point Symmetry	Molecule*	n(Si-O)			n'(Si-O)		
		Si-O(1)*	Si-O(2)	Si-O(3)	Si-O(1)	Si-O(2)	Si-O(3)
T_d	a	0.906			-0.029		
	b	0.857			-0.112		
C_{3v}, α = 117°	c	0.888	0.836		-0.100	-0.117	
114°		0.877	0.846		-0.104	-0.127	
111°		0.864	0.854		-0.109	-0.113	
108°		0.849	0.859		-0.115	-0.111	
105°		0.833	0.861		-0.122	-0.111	
102°		0.815	0.861		-0.130	-0.111	
114°	d	0.864	0.724		-0.021	-0.048	
114°	e	0.864	0.720		-0.021	-0.048	
C_{2v}, α = 117°	f	0.866		0.843	-0.108		-0.116
114°		0.862		0.850	-0.110		-0.115
C_v	g	0.880	0.835	0.847	-0.103	-0.122	-0.117
	h	0.919	0.821	0.852	-0.017	-0.051	0.041

* Molecular letter-labels and oxygen number-labels correspond to those given in Figure 1. n(Si-O) and n'(Si-O) values are not repeated for the symmetry related bonds.

tion in the apical bond increases non-linearly with a concomitant decrease in the overlap population of the basal bonds, predicting that short bonds will be involved in wider O–Si–O angles. The curve for the basal bond is not symmetrical with the curve for apical bond; instead n[Si–O(apical)] and n[Si–O(basal)] follow two separate trends, which reflect the differing MO environments along the basal apical bond directions. The different n(Si–O) trends in Figure 4 appears to corroborate Hoffmann's (1966) view that there need not be a single bond order – bond population relationship between two given atoms having different environments.

Examination of the c_{kj} and S_{ij} matrices obtained in the EHMO calculations suggest that such changes in overlap populations with tetrahedral angles (Fig. 3) can be rationalized in terms of changes in the non-equivalent hybridization characteristics of the central Si atom (see appendix). In order to gain further insight into this problem, the total Hückel energy for a silicate ion (C_{3v} symmetry) (1) with all Si–O = 1.63Å, (2) with Si–O(apical) = 1.58, Si–O (basal) = 1.65Å, and (3) with Si–O(apical) = 1.65 and Si–O (basal) = 1.58Å was calculated as a function of the α angle (Fig. 5). Indeed we find that when all Si–O bond lengths are equal the Hückel $E_{\min}$ is at 109.47°, but when the apical bond is shorter than the basal bonds, $E_{\min}$ shifts to a wider O(apical)– Si–O(basal) angle (α = 111°)

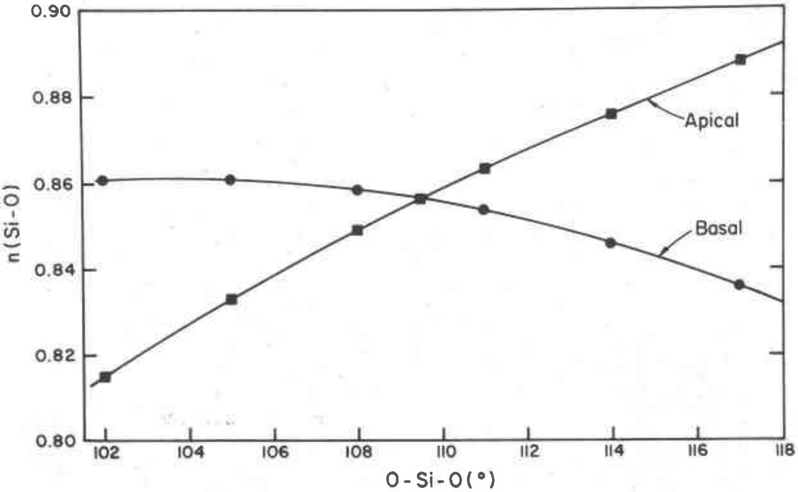

FIG. 4. The variation of n(Si–O) with α = O(apical)–Si–O(basal) angle for a series of orthosilicic acid molecules having C_{3v} symmetry. In the calculation the Si(3d) orbitals were used and all Si–O were assumed equal (1.63Å).

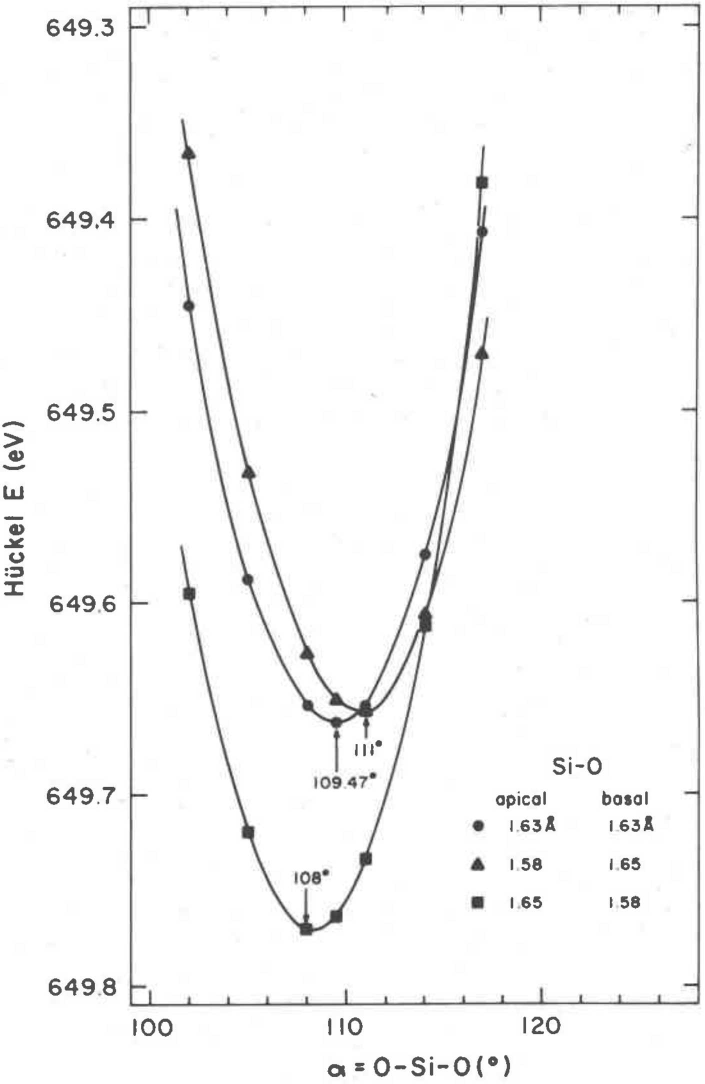

FIG. 5. Plot of total Hückel energy of a silicate ion (C_{3v} symmetry) as a function of α = O(apical)–Si–O(basal) angle for the three cases indicated in the figure, calculated using Si(*sp*) basis.

and when the basal bonds are shorter than apical bond, E_{min} shifts to a narrower O(apical)–Si–O(basal) angle (α = 108°) in conformity with the n(Si–O) predictions.

In silicate structures, silicate tetrahedra with C_{3v} point symmetry are rare. The pyrosilicate ion in $Ba_3Si_4Nb_6O_{26}$ structure (Shannon and Katz, 1970) has silicon in C_3 point symmetry, with three O(1)–Si–O(4) angles = 113° and three O(4)–Si–O(4) angles = 105.7°; the Si–O(1) distance (1.599Å) is shorter than the Si–O(4) distance (1.629Å)—an observation that is consistent with the EHMO predictions. The n(Si–O) vs. α curve in Figure 4 suggests that n[Si–O(1)] ~ 0.872 and that n[Si–O(4)] ~ 0.850; inserting these values into equation (10), the estimated distances [Si–O(1) = 1.612, Si–O(4) = 1.638Å] are in the right direction. The silicate tetrahedron in humite minerals has approximate C_{3v} point symmetry (actual point symmetry is C_v). In chondrodite (Gibbs, Ribbe and Anderson, 1970) for example, the three O–Si–O angles involving the short (1.617Å) Si–O(4) bond are wider (*ca.* 115°) than those (*ca.* 103°) associated with longer Si–O bonds (*ca.* 1.64Å).

The *trends* in bond populations appear to be but slightly affected by the spatial distribution of the four H atoms. For example, calculations with three basal H atoms in an edge–sharing configuration and the apical H making a linear or bent Si–O–H bond (Figs. 1d and 1e, Table 3) show that n[Si–O(apical)] is still larger than n[Si–O (basal)]. When the Si–O–H linkages are *non–linear* n(Si–H) values are positive, suggesting that hydrogen atoms cannot be realistically used to simulate the M–site cations of silicate minerals.

ORTHOSILICIC ACID (C_{2v} POINT SYMMETRY)

Results for two sets of hypothetically distorted H_4SiO_4 tetrahedra with C_{2v} point symmetry are given in Table 3. The two bonds, Si–O(1) and Si–O(2), that enclose the widest O–Si–O angle show a greater overlap population than the remaining two bonds, Si–O(3) and Si–O(4), predicting that Si–O(1) and Si–O(2) bonds should be shorter than Si–O(3) and Si–O(4). The geminal populations of the Si–O(3) and Si–O(4) bonds are larger than in the other two bonds also suggesting that Si–O(3) and Si–O(4) should be longer than Si–O(1) and Si–O(2).

The silicate tetrahedra in benitoite, Na_2SiO_3, and several other structures have approximate C_{2v} point symmetry. In benitoite (Fischer, 1969) the two short (1.605Å) Si–O(2) bonds enclose the widest (113.3°) O–Si–O angle, and the longer Si–O(1) = 1.630 and Si–O(1′) = 1.648Å bonds enclose a narrow angle (107.1°). In Na_2SiO_3

(McDonald and Cruickshank, 1967) the two short Si–O(1) = 1.592Å bonds also enclose the widest (116.9°) tetrahedral angle and the two long Si–O(2) = 1.677 and Si–O(2′) = 1.668Å bonds enclose a narrower (103.1°) angle. Because the observed O–Si–O angles in Na_2SiO_3 structure are close to one of our hypothetically distorted tetrahedron (Fig. 1f, Table 3—row 11) we used the calculated n(Si–O) values to estimate the bond length changes for the distorted tetrahedron in Na_2SiO_3 structure. Equation (10) estimates Si–O(1) $\simeq$ 1.619 and Si–O(2) = 1.646Å both of which are in the right direction as observed in Na_2SiO_3.

ORTHOSILICIC ACID (C_v POINT SYMMETRY)

A silicate tetrahedron with C_v point symmetry can assume several different types of tetrahedral angular distortions. The observed tetrahedral distortions in beryl, topaz, olivine, and $Er_2Si_2O_7$ represent some of the different kinds of distortions within the constraints of C_v point symmetry. The hypothetical H_4SiO_4 molecule we have chosen for EHMO study represents but one of the different types of possible distortions in C_v point symmetry and corresponds to the observed distortions in olivines. The bond overlap and the geminal populations obtained for (1) orthosilicic acid (C_v) where Si–O–H links are linear, (2) orthosilicic acid (C_v) where three basal H atoms are in an edge-sharing configuration and apical Si–O–H line linear, and (3) orthosilicic acid (C_v) as in (2) but with the apical Si–O–H link bent, are given in Table 3. In all three cases, the Si–O bond strengths show three separate populations; the Si–O(1) apical bond is the strongest, the Si–O(2) basal bond weakest, and the Si–O(3), Si–O(4) bonds are of intermediate strength. The relative magnitudes of n'(Si–O) conform to the n(Si–O) predictions, and the largest geminal population is in the Si–O(2) bond for which the bond overlap population is the least. In general, as the $\langle O\text{–}Si\text{–}O\rangle_3$ angle (mean of three O–Si–O angles involving a common bond) widens the bond overlap population of the common bond increases, the geminal population decreases. This prediction is consistent with the observed $\langle O\text{–}Si\text{–}O\rangle_3$ angles and Si–O distances in, for example, forsterite.

	Hypothetical tetrahedron			Forsterite (Brown & Gibbs, in prep.)	
bond	$\langle O\text{–}Si\text{–}O\rangle_3$	n(Si–O)	n'(Si–O)	$\langle O\text{–}Si\text{–}O\rangle_3$	distance
Si–O(1)	115.0°	0.880	−0.103	115.4°	1.614Å
Si–O(3)	108.3	0.847	−0.117	107.5	1.635
Si–O(2)	106.3	0.835	−0.122	106.0	1.654

Equation (10) estimates the right observed order of Si–O distances as Si–O(1) = 1.603, Si–O(3) = 1.642, and Si–O(2) = 1.656Å despite the assumption in the calculation that all Si–O = 1.63Å.

EHMO PREDICTIONS WITH AND WITHOUT 3*d* ORBITALS ON Si

The bond overlap and geminal populations obtained with the *spd* basis for the distorted $(SiO_4)^{4-}$ ions are compared with those obtained with only *sp* basis on Si (Table 4). Whether or not the 3*d* orbitals are included on Si, the EHMO predictions are identical. The type of calculations presented in this paper is not designed to prove whether silicon "uses" its 3*d* orbitals anymore than it proves that silicon "uses" its 3*s* and 3*p* orbitals in bonding with oxygen. Instead the EHMO calculations provide a means for rationalizing bond length variations as a function of the geometrical characteristics (the size of O–Si–O, Si–O–Si angles) of the SiO_4 ions or of their polymerized forms. On the other hand, it should be noted that the *ab initio* calculation for orthosilicic acid strongly supports the thesis for Si(3*d*) participation in the composition of Si–O bond, because (1) the electronic population analysis show considerable 3*d*–orbital involvement in the MOs, (2) the total energy of the molecule is lowered by 16.27eV when the 3*d* orbitals are included in the calculation, and (3) the calculated $L_{2,3}$ X–ray fluorescence spectra bears a very close similarity to the observed spectra of silica glass only when the Si(3*d*) orbitals are included (Collins *et al.*, 1972; Gibbs *et al.*, 1972). Moreover, it must be noted that SCF calculations by Boer and Lipscomb (1969) suggest that even in the SiH_4 molecule the Si3*d* contribution is large enough to be classified as chemically significant (Coulson, 1969, Bartell *et al.*, 1970).

THE IONIC CHARACTER OF THE Si–O BOND

An electronegativity difference between Si and O of 1.7 (Pauling's scale) indicates that the Si–O bond cannot be considered as either 'largely ionic' or 'largely covalent' but is best described as a *heteropolar* bond. Accordingly, calculations based on a purely ionic model cannot be expected to satisfactorily predict the conformational geometries of SiO_4 ions in silicate structures. Moreover, meaningful results from ionic–model calculations require an *a priori* knowledge of the actual charges on the ions as well as a knowledge of their distribution in the structure. Furthermore, any attempt to determine the charge distribution in a structure with heteropolar bonds must resort to quantum mechanics (Hinze, 1970). However, there appears to be a belief among some mineralogists that the Si–O bond can be adequately described by

Table 4. Electronic population analyses: a comparison of results obtained using sp basis and spd basis sets for the ideal and distorted $(SiO_4)^{4-}$ ions, (all Si-O distances at 1.63Å).

	Bond Populations						Geminal Populations					
	sp			spd			sp			spd		
Point Symmetry	Si-O(1)	Si-O(2)	Si-O(3)	Si-O(1)	Si-O(2)	Si-O(3)	Si-O(1)	Si-O(2)	Si-O(3)	Si-O(1)	Si-O(2)	Si-O(3)
T_d	0.496			0.906			-0.029			-0.029		
C_{3v}	0.510	0.490		0.927	0.895		-0.023	-0.033		-0.023	-0.034	
C_{2v}	0.503		0.488	0.915		0.892	-0.027		-0.034	-0.026		-0.034
C_v	0.518	0.473	0.488	0.931	0.883	0.896	-0.020	-0.044	-0.036	-0.021	-0.038	-0.034

an ionic model. This presumably arises from the observation that Pauling's electrostatic charge units, $\zeta(\mathrm{O})$, can be used to predict the variation of the Si–O bond lengths in structures where the oxygen atoms are not all charge balanced.

Pauling's electrostatic valence rule that $\zeta(\mathrm{O})$ should exactly or nearly equal the "valence" of oxygen (with the sign changed) is a condition that tends to minimize the potential energy of the resulting configuration (Pauling, 1929; Bragg, 1930; and Zachariasen, 1963). By definition $\zeta(\mathrm{O})$ simulates the electrostatic attractive potential acting on an oxyanion, $U(\mathrm{O})$,

$$\zeta(\mathrm{O}) = \sum_i s_i = \sum_i \frac{z_i}{\nu_i} \approx U(\mathrm{O}) = \sum_i \frac{q_i q_j}{r_{ij}} \tag{9}$$

where s_i are the electrostatic bond strengths, z_i the nominal valences and ν_i the coordination number of cations bonded to the oxygen, and where q_i and q_j are the charges of the constituent ions (one of them, that of oxygen) separated at internuclear distances r_{ij}. In Pauling's approximation the Si–O tetrahedral bond has a constant electrostatic bond strength of 1.0 in all structures! The observed variation of $\zeta(\mathrm{O})$ reflects largely the changes in ν_i of a given M–site cation and to a lesser degree arises from site–occupancy disorder. However, $\zeta(\mathrm{O})$ does not take into account the non–uniform charge distribution in complex structures. Electronic charge distribution analyses based on SCF MO calculations (*cf.* Hinze, 1970; Bader, Keaveny, and Cade, 1967) suggest that the residual charge on atoms depends both on the nature of bonded atoms and the bond types involved. Our calculations indicate that residual charges on Si and O vary as a function of O–Si–O angles, which is consistent with our foregoing observation that n(Si–O) is a function of O–Si–O angles. Mulliken (1955) has suggested that the *ionic bond order* of a heteropolar bond may be obtained from

$$p_{\text{ionic}}\,(\mathrm{Si\text{–}O}) = -Q(\mathrm{Si})Q(\mathrm{O})[a_o/r(\mathrm{Si\text{–}O})], \tag{10}$$

a relation that bears a close similarity with Pauling's electrostatic bond strength, s_i, and the Coulombic interaction energy, $q_i q_j/r_{ij}$, and where a_o = 0.529Å, the Bohr radius. Even though net EHMO charges are not absolute (Richards and Horsley, 1970), they may be expected to predict a trend in the ionic character of the Si–O bond for a series of conformationally related silicate ions. In Table 5 the calculated net charges Q(Si), Q(O), and ionic bond orders p_{ionic} (Si–O) are listed for a series of H_4SiO_4 tetrahedra (C_{3v} symmetry, all Si–O = 1.63Å) with various O–Si–O angles. These data indicate that Q[O(apical)], Q(Si) as well as p_{ionic} [Si–O(apical)] increase with decreasing O(apical)–Si–O (basal) angle. This result is consistent with the not uncommon observation that the apical Si–O bonds (not involved in shared tetrahedral edges) which enclose wider O–Si–O angles at Si are often shorter. In structures where the oxygen atoms are not all charge balanced, $\zeta(\mathrm{O})$ for the 'apical' bonds are often less than 2.0, implying that the charges on these oxygen are overestimated in Pauling's approximation. Our calculations suggest that valence–balancing can be achieved by a charge density transfer to the apical bond (as evinced by larger n(Si–O) when α is larger than β) resulting in a smaller net charge on O(apical) than on O(basal). The orbital energies of longer Si–O bonds are relatively higher than those of shorter bonds, whereas the net charges on oxygen atoms and ionic bond orders associated with longer bonds are relatively larger. This suggests that the loss of covalent bond energy in the longer Si–O bonds could in part be balanced by an increase in the ionic bond energy.

THE ORIGIN AND EFFECT OF ANGULAR DISTORTIONS

In the extended Hückel picture, the ideal (T_d) H_4SiO_4 molecule has the lowest energy (Fig. 6). However, this does not necessitate that the ground state configuration of an SiO_4 tetrahedron in a *crystal* will exhibit T_d point symmetry when bond lengths are allowed to vary in response to angular distortions; in fact, SiO_4 tetrahedra with T_d point symmetry rarely occur in silicates whereas distorted ones are commonplace. The forces that tend to distort an SiO_4 tetrahedron are well known from the classical work of Pauling (1929; 1960). The C_{3v}, C_{2v}, and C_v type distortions discussed above are very common in silicates and usually result from shortening of edges shared between polyhedra

Table 5. The net atomic charges and ionic bond orders from the EHMO calculations for the H_4SiO_4 molecules of $\underline{C}_{3v}$ symmetry. All Si-O = 1.63Å.

	net charges (e units)			ionic bond orders (a.u.)	
α	$\underline{Q}_{Si}$	$\underline{Q}_{O(apical)}$	$\underline{Q}_{O(basal)}$	Si-O(apical)	Si-O(basal)
117°	1.473	−0.692	−0.749	0.3308	0.3581
114	1.459	−0.706	−0.739	.3343	.3499
111	1.451	−0.720	−0.732	.3391	.3447
109.47	1.451	−0.729	−0.729	.3433	.3433
108	1.452	−0.737	−0.726	.3473	.3421
105	1.458	−0.754	−0.723	.3568	.3421
102	1.472	−0.773	−0.721	.3693	.3444

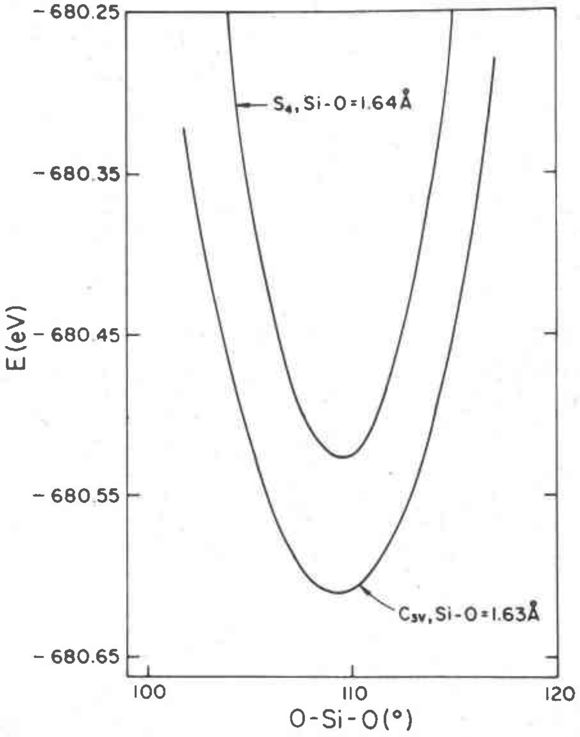

FIG. 6. Plot of total Hückel energy of orthosilicic acid as a function of O–Si–O angles [O(apical)–Si–O(basal) angle for molecule with C_{3v} point symmetry, and O–Si–O angle bisected by the $\bar{4}$ axis for the case of S_4 point symmetry]. When all Si–O = 1.63, the energy minimum for a distorted (C_{3v} or S_4) orthosilicic acid molecule occurs at > O–Si–O = 109.47°.

as expected from electrostatic forces between charged ions. In complex silicate structures the nature of X–O bonds (X = cation) vary from what may be qualitatively described as 'largely ionic' (Li–O, K–O, etc.) to heteropolar (Si–O, Al–O, etc.). When X–O bonds within a polyhedron are largely ionic, competing attractive and repulsive electrostatic forces can also cause angular distortions in the coordination polyhedra (*cf.* Baur, 1961; Hoard and Silverton, 1963; Kepert, 1965). Polymerization of silicate ions coupled with a bending of Si–O–Si as well as O–Si–O angles to fit the polymerized group with other polyhedra in the structure is another cause for tetrahedral (polyhedral) distortions (*cf.* Fig. 4 of Louisnathan and Smith, 1971). Thus distortions are dictated to a polyhedron, in our case the silicate ion, by the crystal chemistry of the entire crystal structure. The slight increase in energy accompanying the distorted configuration is compensated by the removal of certain degeneracies in the symmetric configuration whereby certain bonds shorten and others lengthen. In his paper on *d–p* π–bonding, Cruickshank (1961) proposed a simple rule that the average Si–O distance within a tetrahedron is approximately constant at about 1.63Å [slightly shorter (1.61Å) for framework silicates as reported by Smith and Bailey (1963)], so that as one or more Si–O bonds shorten the others lengthen to preserve the average. Our calculations appear to have found a justification for the above rule. Indeed the mean n(Si–O) for all of the distorted tetrahedra considered (Figs. 1c, f, and g) is 0.854, which compares well with the n(Si–O) = 0.857 for the T_d tetrahedron with Si–O = 1.63Å.

CONCLUSION

The LCAO–EHMO calculation for orthosilicic acid gives results that bear a reasonably close similarity with *ab initio* calculation on the same molecule. Moreover, our results suggest that the n(Si–O) obtained in the EHMO approximation can be used to order and classify the Si–O bond length variations. A mechanism whereby bond lengths can vary as a function of O–Si–O angles has been expounded within the framework of the extended Hückel theory. When angular distortions are present, overlap populations of *both* the σ– and the π–systems are perturbed, and any distortion from the ideal T_d geometry appears to increase the role of $3p$–$2p$ π–bonding in the tetrahedron. In general, our calculations suggest that the strongest (hence short) bonds will be involved in the wider O–Si–O angles, and the weakest (hence long) bonds with the narrower ones. This prediction is also consistent with the bond–pair repulsive mechanism proposed by Gillespie (1963). The bond strength perturbation mechanism explained here is not restricted to the SiO_4 tetrahedron alone but it can easily be extended to other coordination polyhedra. The extended Hückel picture of chemical bonding is by no means an ultimate description of the Si–O bond but it predicts results that are in reasonable agreement with experimental observation as was qualitatively shown in the preceeding pages. Results of EHMO calculations on actual observed structures will be presented elsewhere (Gibbs *et al.*, 1972; Louisnathan and Gibbs, 1972a and 1972b).

APPENDIX: EXTENDED HÜCKEL MOLECULAR ORBITALS FOR ORTHOSILICIC ACID C_{3v} POINT SYMMETRY

For orthosilicic acid with α greater than β (Fig. 1c) the n[Si–O (apical)] calculates to be larger than n[Si–O (basal)]. It was noted that such a difference

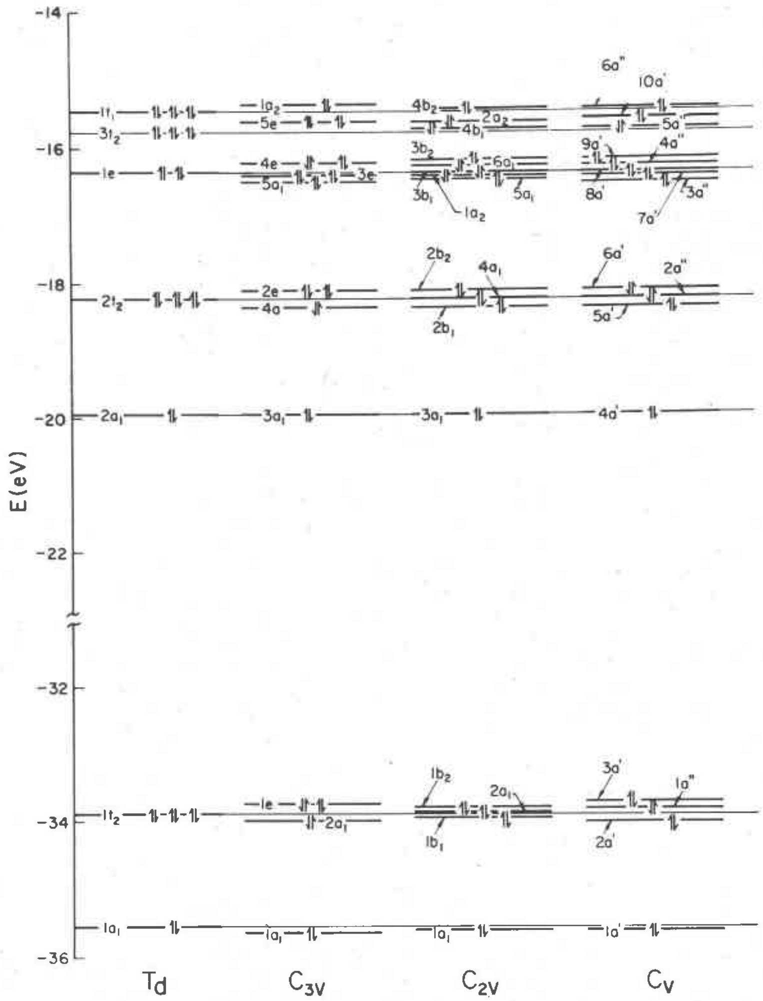

FIG. 7. Walsh-Mulliken-type diagram correlating the MO energy levels (*spd* basis) of a distorted orthosilicic acid molecule with those of an ideal tetrahedron. All Si–O = 1.63Å; for C_{3v}, $\alpha = 117°$; for C_{2v}, $\alpha = 117°$, $\beta = 109.4°$, and γ 102°; and for C_v O–Si–O angles as in Fig. 1g. In this figure the numerical prefixes of MOs follow the EHMO valence orbital scheme and not an all electron MO scheme. Thus for example $1a_1$ (T_d) in this figure would correspond to $4a_1$ of *ab initio* calculations (see Table 2).

in overlap populations of bonds within the same tetrahedron can be rationalized in terms of non-equivalent hybridization characteristics of Si atom. A detailed description of such characteristics may facilitate an understanding of the relationship between bond angles and bond lengths within a tetrahedron. As the EHMO calculations lack the rigor of *ab initio* SCF–MO calculations only qualitative significance should be attached to the following description.

Figure 7 compares the EHMO energy levels of orthosilicic acid in ideal and distorted (C_{3v}; $\alpha = 117°$) conformations. The first six energy levels, $1a_1$, to $2e$ of H_4SiO_4 (C_{3v}) represent the σ–bonding molecular orbitals, and correspond to the first four levels of the ideal tetrahedron with some of their orbital degeneracies removed because of angular distortions. The $1a_1$ (C_{3v}) is slightly lower in energy

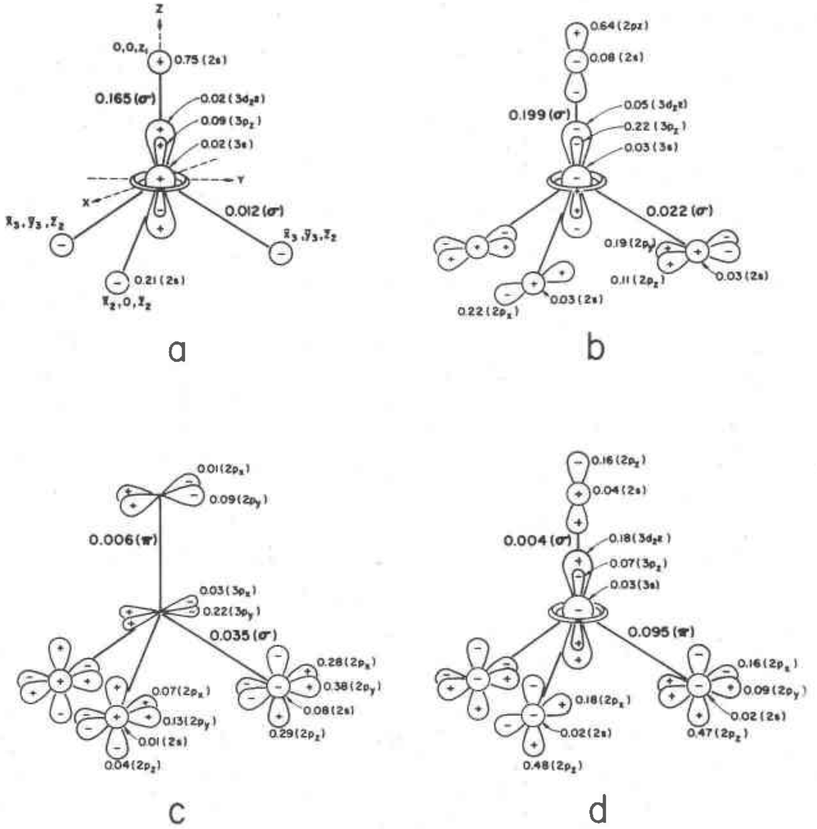

FIG. 8. Schematic representation of the STO–AO components of the molecular orbitals for a orthosilicic acid molecule of C_{3v} symmetry with α 117° and all Si–O = 1.63Å. Hydrogen orbitals are omitted. (a) represents the AO components of the $2a_1$ MO, (b) of the $4a_1$ MO, (c) of the $2e$ MO with $3d$ components suppressed, and (d) of the $5a_1$ MO. The bold-face numbers indicate the partial overlap population that these MOs contribute to the total n(Si–O).

than its corresponding $1a_1$ (T_d), a consequence of increased overlap resulting from the mixing of $3s$ and $3p_z$ orbitals. The $2a_1$ MO is of the form,

$$[0.02(3s) + 0.09(3p_z) + 0.02(3d_{z^2})]_{\mathrm{Si}} + [0.75(2s)]_{\mathrm{O\,(apical)}} - 0.21[(2s_2) + (2s_3) + (2s_4)]_{\mathrm{O\,(basal)}}$$

indicating a relatively stronger σ–bond for the apical oxygen than for the basal ones (Fig. 8a). In the $1e$ MO which is slightly higher in energy than $2a_1$, only the basal oxygen atoms participate in bonding.

Together the $2a_1$ and $1e$ MOs represent a condition where the apical Si–O bond gains more strength relative to the basal Si–O bonds via a *3spd–2s* type σ–bond. The $4a_1$ (Fig. 8b) and $2e$ MOs also represent a similar situation; however, the σ–bond involved here is of *3spd–2sp* type. In the doubly degenerate $2e$ level, $3p_x$ as well as $3p_y$ participate with the same sign as the $2p_x$ and $2p_y$ of the apical oxygen indicating $3p$–$2p$ π–bonding (Fig. 8c), whereas for the basal oxygen atoms the $2e$ MOs are σ–bonding type as in $2t_2(T_d)$. With ideal tetrahedral angles the $3p$–$2p$ π–bonding interactions are weak whereas with C_{3v} type of distortion, they are relatively stronger for the apical bond.

The $5a_1$, $3e$, $4e$, and $5e$ energy levels constitute orbitals that are predominantly π–bonding in the H_4SiO_4 molecule with C_{3v} point symmetry. In the $5a_1$ MO the $p\pi$ orbitals of basal oxygen atoms mate the $(3s + 3p_z + 3d_{z^2})$ combination in π–bonding while a $2p\sigma$ orbital of the apical oxygen mates the same combination in σ–bonding, a $3d$–$2p$ σ–bond (Fig. 8d). The $3e$ and $4e$ orbitals are similar in character to the $1e(T_d)$ and $2t_2(T_d)$ MOs where orbitals of *all* the oxygen atoms mate the $d(e)$–orbitals $(d_{xz}, d_{x^2-y^2}, d_{yz}$, and $d_{xy})$ in d–p π–bonding. Any deviation from the ideal T_d geometry imparts comparable roles to *all five* $3d$ orbitals of Si in d–p π–bonding. The $5e$ level is a weakly π–bonding level for the basal oxygen atoms and an antibonding level for the $3p$–$2p$ π–bonding MO of the apical oxygen. The $1a_2$ nonbonding MO constitutes a linear combination of atomic orbitals from only the basal oxygen atoms. Thus the strengthening of the Si–O(apical) relative to Si–O(basal) is accomplished by a relative increase in the σ– as well as π– overlaps, $S_{\mathrm{Si,O(apical)}}$, and consequent lowering in ϵ_k of the MOs involving the apical oxygen. The magnitudes of splitting, $\Delta\epsilon_k$, obtained in the EHMO calculations are not absolute; however, the symmetry aspects of the MOs given above are consummate. Furthermore, an *ab initio* SCF calculation will yield the same kind of symmetry orbitals because the MOs must be classifiable according to the irreducible representations of the molecule's point group. Indeed, a great deal of the success of the EHMO predictions are attributed to *orbital symmetry* considerations (Allen, 1970).

ACKNOWLEDGMENTS

This paper has benefited greatly from constructive criticisms of our preliminary ideas particularly by L. S. Bartell and D. R. Peacor of the University of Michigan, L. C. Allen and G. E. Brown, Jr. of Princeton University, and D. W. J. Cruickshank of the University of Manchester Institute of Science and Technology. Professor Cruickshank is gratefully acknowledged for valuable discussion on bonding theory during a recent visitation to our department and for copies of the computer output of the *ab initio* calculations for the silicate ion and for orthosilicic acid. It is a pleasure to acknowledge the National Science Foundation for research grants GA–12702, GA–30864X, and GU–1392, which contributed significantly to the support of the study; and the Research Division at VPI & SU for funds used to complete a portion of the MO calculations.

S. J. L. acknowledges the departmental grant GU-1392 for support in the form of research associateship.

References

Allen, L. C. (1970) Why three-dimensional Hückel theory works and where it breaks down. *In* O. Sinanoğlu and K. B. Wiberg, eds. *Sigma Molecular Orbital Theory,* Chap. VI-2, Yale University Press.

———, and J. D. Russell (1967) Extended Hückel theory and the shape of molecules. *J. Chem. Phys.* **46**, 1029–1037.

Bader, R. F. W., I. Keaveny, and P. E. Cade (1967) Molecular charge distributions and chemical binding. II. First-row diatomic hydrides, AH. *J. Chem. Phys.* **47**, 3381–3402.

Bartell, L. S., L. S. Su, and H. Yow (1970) Lengths of phosphorus-oxygen and sulfur-oxygen bonds. An extended Hückel molecular orbital examination of Cruickshank's d_π–p_π picture. *Inorg. Chem.* **9**, 1903–1912.

Basche, H., A. Viste, and H. B. Gray (1965) Valence orbital ionization potentials from atomic spectral data. *Theoret. Chim. Acta* **3**, 458–464.

Baur, W. H. (1961) Über die Verfeinerung der Kristallstrukturbestimmung einiger Vertreter des Turiltyps. III. Zur Gittertheorie des Rutiltyps. *Acta Crystallogr.* **14**, 209–213.

——— (1970) Bond length variation and distorted coordination polyhedra in inorganic crystals. *Trans. Amer. Crystallogr. Ass.* **6**, 125–155.

——— (1971) The prediction of bond length variations in silicon-oxygen bonds. *Amer. Mineral.* **56**, 1573–1599.

Boer, F. P., and W. N. Lipscomb (1969) Molecular SCF calculations for SiH_4 and H_2S. *J. Chem. Phys.* **50**, 989–992.

Bokii, N. G., and Y. T. Struchkov (1968) Structural chemistry of organic compounds of the nontransition elements of Group IV (Si, Ge, Sn, Pb). *Zh. Strukt.: Khim.* **9**, 722–765.

Boyd, D. B., and W. N. Lipscomb (1969) Electronic structures for energy rich phosphates. *J. Theoret. Biol.* **25**, 403–420.

Bragg, W. L. (1930) The structure of silicates. *Z. Kristallogr.* **74**, 237–305.

Brown, G. E., and G. V. Gibbs (1969) Oxygen coordination and the Si–O bond. *Amer. Mineral.* **54**, 1528–1539.

———, and ——— (1970) Stereochemistry and ordering in the tetrahedral portion of silicates. *Amer. Mineral.* **55**, 1589–1607.

———, ———, and P. H. Ribbe (1969) The nature and variation in length of the Si–O and Al–O bonds in framework silicates. *Amer. Mineral.* **54**, 1044–1061.

Cannillo, E., G. Rossi, and L. Ungaretti (1968) The crystal structure of macdonaldite. *Accad. Naz. Lincei,* **45**, 399–414.

Clementi, E., and D. L. Raimondi (1963) Atomic screening constants from SCF functions. *J. Chem. Phys.* **38**, 2686–2689.

Collins, G. A. D., D. W. J. Cruickshank, and A. Breeze (1972) *Ab initio* calculations on the silicate ion, orthosilicic acid and their $L_{2,3}$ X-ray spectra. *J. Chem. Soc., Faraday Trans. II,* **68**, 1189–1195.

Cotton, A. F., and G. Wilkinson (1966) *Advanced Inorganic Chemistry.* John Wiley and Sons, New York, N.Y., 69–72.

Coulson, C. A. (1969) *d* electrons and molecular bonding. *Nature,* **221**, 1106–1110.

——— (1970) σ–bonds; π–bonds. *In* H. Eyring, ed. *Physical Chemistry, An Advanced Treatise.* Academic Press, New York.

Cruickshank, D .W. J. (1961) The role of 3d–orbitals in π–bonds between (a) silicon, phosphorus, sulfur, or chlorine and (b) oxygen or nitrogen. *J. Chem. Soc. (London),* p. 5486–5504.

Fischer, K. (1969) Verfeinerung der Kristallstruktur von Benitoit BaTi[Si_3O_9]. *Z. Kristallogr.* **129,** 222–243.

Fyfe, W. S. (1954) The problem of bond type. *Amer. Mineral.* **39,** 991–1004.

Gibbs, G. V., P. H. Ribbe, and C. P. Anderson (1970) The crystal structures of the humite minerals II. Chondrodite. *Amer. Mineral.* **55,** 1182–1194.

———, M. M. Hamil, S. J. Louisnathan, L. S. Bartell, and H. Yow (1972) Correlations between Si–O bond length, Si–O–Si angle and bond overlap populations calculated using extended Hückel molecular orbital theory. *Amer. Mineral.* **57,** 1578–1613.

Gillespie, R. J. (1963) The valence–shell electron–pair repulsion (VSEPR) theory of directed valence. *J. Chem. Ed.* **40,** 295–301.

Hinze, J. (1970) Heteropolar bonds. *In* H. Eyring, ed. *Physical Chemistry, An Advanced Treatise.* Academic Press, New York, Chap. 4.

Hoard, J. L., and J. V. Silverton (1963) Stereochemistry of discrete sight–coordination. I. Basic analysis. *Inorg. Chem.* **2,** 235–249.

Hoffmann, R. (1963) An extended Hückel theory. I. Hydrocarbons. *J. Chem. Phys.* **39,** 1397–1412.

——— (1966) Extended Hückel theory-VI, Excited states and photochemistry of Diazirines and Diazonrethanes. *Tetrahedron,* **22,** 539–545.

Kepert, D. L. (1965) The stereochemistry of eight–co–ordination. *J. Chem. Soc.* **1965,** 4736–4744.

Lazarev, A. N. (1964) Polymorphism of molecules and complex ions in oxygen compounds of silicon and phosphorus report I. Nature of the Si–O–Si bonds and values of the valence angles of oxygen. *Izv. Akad. Nauk SSSR, Ser. Khim.* **2,** 235–241.

Louisnathan, S. J., and G. V. Gibbs (1971) A comparison of Si–O distances in olivines with bond overlap populations as predicted by the extended Hückel molecular orbital (EHMO) theory. [abstr.] *Geol. Soc. Amer. Abstr. Programs,* **3,** 636.

———, and ——— (1972a) Aluminum–silicon distribution in zunyite. *Amer. Mineral.* **57,** 1089–1108.

———, and ——— (1972b) Variation of Si–O distances in olivines, sodamelilite and sodium metasilicate as predicted by semiempirical molecular orbital calculations. *Amer. Mineral.* **57,** 1643–1663.

———, and J. V. Smith (1971) Crystal structure of tilleyite: Refinement and coordination. *Z. Kristallogr.* **132,** 288–306.

McDonald, W. S., and D. W. J. Cruickshank (1967) A reinvestigation of the structure of sodium metasilicate, Na_2SiO_3. *Acta Crystallogr.* **22,** 37–43.

Mitchell, J. T., F. D. Bloss, and G. V. Gibbs (1971) Examination of the actinolite structure and four other C2/m amphiboles in terms of double bonding. *Z. Kristallogr.* **133,** 273–300.

Mulliken, R. S. (1950) Overlap integrals and chemical binding. *J. Amer. Chem. Soc.* **72,** 4493–4503.

——— (1951) Overlap and bond power of 2*s,* 2*p*–hybrid orbitals. *J. Chem. Phys.* **19,** 900–912.

——— (1955) Electronic population analysis on LCAO–MO molecular wave functions. I., *J. Chem. Phys.* **23**, 1833–1840. II. Overlap populations, bond orders, and covalent bond energies. *J. Chem. Phys.* **23**, 1841–1846.

Noll, W. (1963) The silicate bond from the standpoint of electronic theory. *Angew. Chem.* **2**, 73–80.

Novak, G. A., and G. V. Gibbs (1971) The crystal chemistry of the silicate garnets. *Amer. Mineral.* **56**, 791–825.

Pauling, L. (1929) The principles determining the structure of complex ionic crystals. *J. Amer. Chem. Soc.* **51**, 1010–1026.

——— (1952) Interatomic distances and bond character in the oxygen acids and related substances. *J. Phys. Chem.* **56**, 361–365.

——— (1939, 1960) *The Nature of the Chemical Bond, 1st and 3rd eds.* Cornell University Press, Ithaca, N.Y.

Richards, W. G., and J. A. Horsley (1970) Ab initio *Molecular Orbital Calculations for Chemists.* Clarendon Press, Oxford, p. 102.

Salem, L. (1966) *Molecular Orbital Theory of Conjugated Systems.* Benjamin, New York.

Shannon, J., and L. Katz (1970) The structure of barium silicon niobium oxide, $Ba_3Si_4Nb_6O_{26}$: A compound with linear silicon–oxygen–silicon groups. *Acta Crystallogr.* **B26**, 105–109.

Slater, J. C. (1963) *Quantum Theory of Molecules and Solids.* Vol. 1, *Electronic Structure of Molecules.* McGraw-Hill, New York.

Smith, J. V., and S. W. Bailey (1963) Second review of Al–O and Si–O tetrahedral distances. *Acta Crystallogr.* **16**, 801–811.

Wolfsberg, M., and L. Helmholz (1952) The spectra and electronic structure of the tetrahedral ions MnO_4^-, CrO_4^{2-}, and ClO_4^-. *J. Chem. Phys.* **20**, 837–843.

Zachariasen, W. H. (1963) The crystal structure of monoclinic metaboric acid. *Acta Crystallogr.* **16**, 385–389.

Manuscript received November 24, 1971; accepted for publication June 29, 1972.